

No Regret Sample Selection with Noisy Labels

Heon Song^{*,†}

Nariaki Mitsuo^{*}

Seiichi Uchida^{*}

Daiki Suehiro^{*,†}

^{*}Kyushu University, Japan

[†]RIKEN AIP, Japan

{heon.song@human., uchida@, suehiro@}ait.kyushu-u.ac.jp

Abstract

Deep neural networks (DNNs) suffer from noisy-labeled data because of the risk of overfitting. To avoid the risk, in this paper, we propose a novel DNN training method with sample selection based on adaptive k -set selection, which selects k ($< n$) samples with a small noise-risk from the whole n noisy training samples at each epoch. It has a strong advantage of guaranteeing the performance of the selection theoretically. Roughly speaking, a regret, which is defined by the difference between the actual selection and the best selection, of the proposed method is theoretically bounded, even though the best selection is unknown until the end of all epochs. The experimental results on multiple noisy-labeled datasets demonstrate that our sample selection strategy works effectively in the DNN training; in fact, the proposed method achieved the best or the second-best performance among state-of-the-art methods, while requiring a significantly lower computational cost.

1. Introduction

Deep neural networks (DNNs) require a large number of “correctly-labeled” samples to achieve high-performance classification [43]. However, it is practically difficult for many CV/PR-related datasets to guarantee the correctness of the attached labels [6, 29]. For example, datasets annotated via crowd-sourcing [37, 42] often become noisy-labeled samples, which contain a certain number of samples with incorrect labels. Beyers et al. [2] point out that ImageNet contains several incorrectly labeled samples, even though each sample in ImageNet is labeled by a careful majority voting scheme among at least 10 workers [5]. Datasets created by automatic data collection and annotation, such as Clothing1M [36], will also contain a large number of incorrectly labeled samples.

A possible remedy for noisy-labeled samples is *sample selection*, which is a method to select a clean subset of training samples (i.e., correctly labeled training samples) from the whole sample set. A typical strategy is co-training, which compares the results from two DNNs to detect the

incorrectly labeled samples, as shown in Fig. 1 (a). This strategy has achieved state-of-the-art performance so far but requires extra computations due to its coupled-DNN structure. Another drawback is that it has no theoretical guarantee on its performance.

We can consider another sample selection strategy by using the idea of k -set, which is a subset of k samples. Fig. 1 (b) shows the most naive k -set-based sample selection strategy; after generating all $\binom{n}{k}$ k -sets exhaustively from the whole training set with n samples, $\binom{n}{k}$ DNNs are trained independently with individual k -sets. If there are more than k clean samples, some DNNs are trained only by clean samples and thus avoid the degradation by incorrectly labeled samples. However, this naive and exhaustive k -set strategy is obviously intractable in practical scenarios with larger n and k .

This paper proposes a method where k -set selection and DNN training by the selected k samples are performed alternately. Let \mathbf{d}_t denote the n -dimensional k -set vector showing the selection at epoch t and $\boldsymbol{\theta}_{t-1}$ denote the n -dimensional *noise-risk vector* whose i th element is the noise-risk of the i th training sample, which is assessed at $t - 1$. The noise-risk is the likelihood that the sample is incorrectly labeled. In the ideal case when $\boldsymbol{\theta}_t$ is highly reliable, we can select the k -set \mathbf{d}_t that minimizes $\mathbf{d}_t \cdot \boldsymbol{\theta}_{t-1}$. However, this greedy strategy does not work because of the difficulty of having a reliable $\boldsymbol{\theta}_t$ during the training process.

We, therefore, design our method to suppress the *total selection risk*, which is defined as $\sum_{t=1}^T \mathbf{d}_t \cdot \boldsymbol{\theta}_t$, as shown in Fig. 1 (c). By achieving a smaller total selection risk at T , we can believe that DNN is trained with less incorrectly-labeled samples *on average* during the entire training process. Due to the online (i.e., non-predictable) nature of the training process, one may imagine that it is difficult to determine \mathbf{d}_t at t while guaranteeing a smaller total selection risk. We prove that it is still possible to achieve a total selection risk smaller than a theoretical bound, based on the theory of *adaptive k -set selection* [33] with *Follow-the-Perturbed Leader* (FPL) algorithm, as discussed later. Hereafter we call the proposed method *training DNN with sample selection based on adaptive k -set selection* (TAKS).

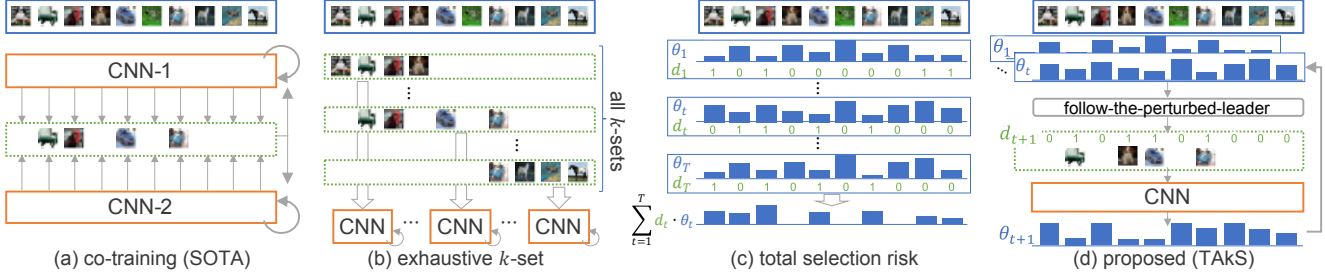


Figure 1: (a) Co-training. (b) The most naive and computationally-intractable k -set selection method. (c) Total selection risk. (d) The proposed method based on adaptive k -set selection. The vectors θ_t and \mathbf{d}_t are the noise-risk vector and the k -hot vector at epoch t , respectively. In (d), the perturbation mechanism in the k -set selection is omitted for simplicity.

Fig. 1 (d) shows TAKS, which has the following three advantages. The first and most important advantage is its theoretical support. Specifically, its performance is theoretically guaranteed in terms of *regret*. Regret is a performance measure and is often used in theoretical machine learning research. In our k -set selection task, the regret R_T is defined as the difference between the actual total selection risk and the minimum total selection risk with the best k -set \mathbf{d}^* . (See Eq. (2) for the formal definition of R_T .) Although \mathbf{d}^* is unknown until T , R_T of TAKS is upper-bounded; this means that the k -set selection by TAKS is not far from \mathbf{d}^* , even under the uncertain online nature of the selection process.

The second advantage is its computational efficiency. TAKS selects an appropriate k -set \mathbf{d}_t from all the $\binom{n}{k}$ k -set candidates with just $O(n)$ time complexity at each t . In addition, TAKS trains a single DNN, whereas the state-of-the-art sample selection methods (i.e., the co-training methods) need to train coupled-DNNs as noted above.

Finally, TAKS achieves the best or near-best classification accuracy, as shown by our experimental results on several benchmark datasets, such as MNIST [15], CIFAR-10, CIFAR-100 [14], and Clothing1M [36], which have often been used in the past studies of noisy-labeled samples. Under various noise settings, TAKS achieves the best or the second-best accuracy and time efficiency among various state-of-the-art sample selection methods [7, 34, 40].

The summary of our main contributions are as follows:

- For learning with noisy-labels, we propose a novel and efficient method, TAKS, which tries to suppress the total selection risk based on the theory of adaptive k -set selection. To the best of our knowledge, TAKS is the first method that utilizes the idea of adaptive k -set selection for noisy-labeled samples.
- We discuss how the theoretical support of TAKS is useful for selecting a promising k -set from noisy-labeled samples. We also prove how the performance of TAKS is guaranteed in terms of the total selection risk.
- The experimental results on multiple noisy-labeled

datasets show that TAKS achieved the best or the second-best performance in not only classification accuracy but also time efficiency among state-of-the-art methods. We also confirmed that TAKS selects more clean samples than the other comparative methods.

2. Related Work

2.1. Learning with noisy labels

Sample selection strategies for noisy-labeled samples

Among the various methods for dealing with noisy-labeled samples, one of the most popular choices is sample selection, which selects clean sample candidates from the whole training sample set. The clear merit of sample selection is that it can totally exclude the unexpected effect of the non-selected incorrectly labeled samples. Moreover, it is also useful to remove irrelevant samples before reusing the sample set for another task.

A widely used sample selection strategy for DNN training is to select samples with small training loss (such as cross-entropy loss for the classification task). ITML [27] considers the samples with a small training loss in the initial epochs to be clean samples. Therefore, it selects samples with small training loss at the end of every epoch and trains the DNN with the samples. Unlike this strategy, iterative learning [32] considers incorrectly labeled samples as outliers and removes the noise using the outlier detection algorithm [3].

Recent state-of-the-art methods take the strategy of co-training, which trains coupled-DNNs simultaneously for clean sample selection [7, 10, 19, 34, 40]. Decoupling [19] selects the samples that the two classifiers predict differently and uses them for training the classifiers. In Co-teaching [7], each of the two classifiers selects the samples with small training loss and then exchanges the samples for training the other classifier. Co-teaching+ [40] uses both ideas of Decouple and Co-teaching. JoCoR [34] tries to make the classification results of two classifiers closer to each other while selecting samples with a small loss. Although these state-of-the-art methods have shown outstand-

ing performance, their coupled-DNN structure requires almost double the computation time and resources than a single DNN training. Moreover, their theoretical justification has not yet been provided.

Other strategies for noisy-labeled data One of the strategies to train a DNN with noisy-labeled data is estimating a label transition matrix [21, 23, 24, 35]. The label transition matrix is a matrix that represents the probability of a label flipping from one class to another. F-correction [24] is a popular method that estimates the label transition matrix to improve the robustness of DNN. It estimates the matrix using a well-trained DNN with noisy-labeled data and trains another DNN by weighting losses using the estimated matrix. This strategy is theoretically well-motivated. However, it is practically difficult to estimate the label transition matrix with many classes. Consequently, the practical performance is not so high, compared with the above sample selection-based methods.

Another strategy is to utilize additional “clean” data [17, 25, 26, 31, 38]. Veit et al. [31] used clean data to train a label cleaning network. Using the label cleaning network, it is possible to clean up noisy-labeled data and train a DNN with the cleaned data. Ren et al. [25] proposed a weighting algorithm to learn with noisy-labeled data. It weighs the training data to reduce the loss of clean validation data. Rodrigues et al. [26] proposed a crowd layer that contains annotator-specific functions. By assigning reliability to the functions, unreliable annotators and annotators’ bias can be avoided. Yao et al. [38] designed a method for improving the existing sample selection method using the AutoML technique. Using clean validation data and its loss, the method searches a proper selection schedule automatically. However, these methods require a lot of time and resources to collect clean data or labels from multiple annotators.

2.2. Adaptive k -set selection

TAKS utilizes the idea of *adaptive k -set selection* [33], which is a task of selecting some good k elements from n elements *repeatedly*. Roughly speaking, the task is to select a good k -set of elements adaptively under the assumption that the temporarily optimal selection can dynamically change in the repeating.

The adaptive k -set selection mainly focuses on theoretical research, and its applicability to real-world tasks has not been demonstrated. In fact, it was originally proposed for theoretical research for the online PCA task [33]. Then, many extended research studies have been proposed [4, 13, 28], and it is still the subject of theoretical research. Therefore, this paper is the first attempt at using adaptive k -set selection for noisy-labeled data.

Algorithm 1 TAKS

1: **Inputs:**

Training samples $(x_1, y_1), \dots, (x_n, y_n)$,
total epochs T , initial DNN f_0 , $k, \eta > 0$

2: **Outputs:**

f_T : trained DNN

3: **Initialize:**

Set \mathbf{d}_1 as an n -dimensional k -hot vector

4: **for** epochs $t = 1, \dots, T$ **do**

5: Obtain f_t by training f_{t-1} with the k -set, \mathbf{d}_t .

6: Update the noise-risk vector $\boldsymbol{\theta}_t = (\theta_{1,t}, \dots, \theta_{n,t})$.

7: Sample the perturbation $r_i \sim \mathcal{N}(0, 1)$ for all i .

8: Select the next k -set of samples:

$$\mathbf{d}_{t+1} = \arg \min_{\mathbf{d} \in \mathcal{D}} \left(\sum_{\tau=1}^t \mathbf{d} \cdot \boldsymbol{\theta}_\tau + \eta \mathbf{d} \cdot \mathbf{r} \right) \quad (1)$$

9: **end for**

3. Training DNN with Sample Selection Based on Adaptive k -set Selection (TAKS)

3.1. Basic settings

We assume the task of training a DNN-based classifier with noisy-labeled samples. Let x_1, \dots, x_n be training samples and y_1, \dots, y_n their labels. Some samples are labeled incorrectly. The goal is to obtain a DNN-based classifier f_T after T epochs and achieve high classification accuracy on a test sample set. Note that, in the popular setup of noisy-labeled samples, the test sample set is not noisy to facilitate the final classification evaluation easier. We also follow the same setup.

Letting f_t denote the DNN after epoch t and \mathcal{D} denote the set of all possible k -sets, the basic procedure of TAKS at epoch t is described as the following three steps (recall Fig. 1 (d)):

1. Select a good \mathbf{d}_t from \mathcal{D} by a selection algorithm.
2. Train f_{t-1} with the k samples in \mathbf{d}_t and get f_t .
3. Assess the noise-risk vector $\boldsymbol{\theta}_t$.

The details of TAKS based on the procedure are shown in Algorithm 1 and described in the later sections. Specifically, for Step 1, we will show a theoretical definition of what is a good selection in Sec. 3.2. We then show a selection algorithm in Sec 3.3. For Step 3, we can use an arbitrary approach, although we expect that the i th element $\theta_{i,t}$ of the noise-risk vector $\boldsymbol{\theta}_t \in [0, 1]^n$ becomes larger when the noise-risk of the i th sample is higher at epoch t . Sec. 5.1 gives a reasonable way to assess $\boldsymbol{\theta}_t$. Note that $\boldsymbol{\theta}_t$ is assessed after training the DNN at Step 2; in other words,

the previous noise-risk vectors $\theta_1, \dots, \theta_{t-1}$ can be used for selecting \mathbf{d}_t .

3.2. Total selection risk and adaptive k -set selection

To achieve high classification performance by the DNN, it is better to select \mathbf{d}_t with less incorrectly-labeled samples at each epoch t . The greedy selection of \mathbf{d}_t with minimum noise-risk (i.e., $\min_{\mathbf{d}_t \in \mathcal{D}} \mathbf{d}_t \cdot \theta_{t-1}$) at each epoch t is not reasonable; this is because the noise-risk vector θ_{t-1} might be quite unstable during training the DNN. For example, $\theta_{i,t}$ can be very large even if $\theta_{i,t-1}$ is very small. It might happen in the DNN training where just one epoch training makes a big change in the evaluation of the i th sample.

To deal with this instability, TAKS aims to suppress the total selection risk $\sum_{t=1}^T \mathbf{d}_t \cdot \theta_t$; this means TAKS aims to suppress the *average* selection risk during $t = 1, \dots, T$. This aim seems reasonable but not straightforward because it is non-predictable at each $t < T$ that the selection at t is surely good for a smaller total selection risk, due to the high instability of θ_t . In other words, we cannot have any ‘‘assumption’’ for predicting the total selection risk from the current selection at t .

Therefore, we consider the selection task as *adaptive k -set selection* [33]. Adaptive k -set selection is defined as a task in which the k -set selection and its evaluation are alternated repeatedly, and thus similar to our selection procedure. The theoretical goal of the adaptive k -set selection is to select $\mathbf{d}_1, \dots, \mathbf{d}_T$ with a guarantee of the small total selection risk for *any* $\theta_1, \dots, \theta_T$. In other words, the adaptive k -set selection task assumes even a very tough situation where θ_t can change drastically at every t and thus is not predictable.

An important and general theoretical highlight of the adaptive k -set selection task is that its *regret* R_T can be upper bounded as:

$$R_T = \sum_{t=1}^T \mathbf{d}_t \cdot \theta_t - \min_{\mathbf{d} \in \mathcal{D}} \sum_{t=1}^T \mathbf{d} \cdot \theta_t, \quad (2)$$

for *any* θ_t (i.e., for any tough situation). The first term is the total selection risk. The second term is the total selection risk when we use *the best selection* $\mathbf{d}^* = \operatorname{argmin}_{\mathbf{d}} \sum_{t=1}^T \mathbf{d} \cdot \theta_t$ at all T rounds. That is, regret means the relative performance (i.e., total selection risk) difference between the best selection and actual selection. The upper-bound of R_T depends on the algorithm to select \mathbf{d}_t at each round. Thus, if we use a selection algorithm that gives a smaller upper bound, we can expect a smaller R_T , that is, good performance similar to the best selection \mathbf{d}^* .

The following three points should be emphasized regarding the above regret upper bound. First, R_T can be bounded theoretically even though the best selection \mathbf{d}^* is only known after the end of the T rounds and thus unknown when we decide \mathbf{d}_t at each $t < T$. Second, R_T

is still bounded even though the noise-risk vector θ_t fluctuates drastically along with t . Third, the upper bound of R_T depends on the choice of the selection algorithm, as noted above.

It should be emphasized again that adaptive k -set selection is a general online selection task, and these theoretical supports hold in arbitrary k -set selection tasks. Therefore these supports also hold our sample selection task for training a DNN. Especially, having a lower regret bound is very meaningful for our task because it indicates that we can expect a performance similar to the best selection \mathbf{d}^* in terms of the total selection risk. (This point is further supported by Corollary 2.)

3.3. Adaptive k -set selection using FPL

The remaining issue is the choice of the sample selection algorithm that gives a lower regret bound. For TAKS, we employ the *Follow-the-Perturbed-Leader* (FPL) [4] as a selection algorithm for adaptive k -set selection, because it gives a good regret bound [4, 13, 28, 33]. FPL is an improved version of the *Follow the Leader* (FTL) algorithm [8], which selects the ‘‘current best’’ k -set \mathbf{d}_t^* at epoch t (i.e., $\mathbf{d}_t^* = \operatorname{argmin}_{\mathbf{d}} \sum_{\tau=1}^t \mathbf{d} \cdot \theta_\tau$.) Although the idea of FTL seems reasonable, it has already been proved that FTL can overfit to tough $\theta_1, \dots, \theta_T$ and cannot have a meaningful regret bound [8]. In contrast, FPL selects k samples based on the perturbed selection risk, in order to avoid FTL’s overfitting and have the regret bound. More precisely, Steps 7 and 8 in Algorithm 1 show the k -set selection algorithm based on FPL, where $\mathbf{r} = (r_1, \dots, r_n)$ is a random vector for the perturbation [4, 11].

3.4. Efficiency and versatility

The major computational cost of TAKS comes from the sample selection steps (Steps 6-8 in Algorithm 1) and the DNN training cost with k samples (Step 5). The former is dominated by the minimization operation in Eq. (1) and efficiently performed just with $O(n)$ computations despite $|\mathcal{D}| = \binom{n}{k}$. The term to be minimized is rewritten as follows: $\left(\sum_{\tau=1}^t \mathbf{d} \cdot \theta_\tau + \eta \mathbf{d} \cdot \mathbf{r} \right) = \left(\sum_{\tau=1}^t \theta_\tau + \eta \mathbf{r} \right) \cdot \mathbf{d}$. Therefore, finding the optimal \mathbf{d} in Eq. (1) is equivalent to finding the elements with the k least perturbed total selection risk in $\left(\sum_{\tau=1}^t \theta_\tau + \eta \mathbf{r} \right)$ and requires $O(n)$ computations for finding the top- k elements from n elements [22]. Consequently, TAKS works efficiently with just $O(n)$ computations and thus can deal with large training sample sets.

Consequently, the latter (Step 5) requires more computations than the former (Steps 6-8) in practice; however, even the latter computation is far more efficient than the standard DNN training. This is because TAKS requires the DNN training cost with k ($< n$) samples instead of n samples.

Algorithm 1 also shows the versatility of TAKS; we can

employ an arbitrary DNN. In the later experiment, we use several different neural networks in TAKS.

4. Theoretical Support of TAKS

In this section, we show that TAKS is theoretically supported by regret-based analysis. Note that our sample selection method generally works with the theoretical support for any sequences of the noise-risk vectors. In other words, to receive the benefit of the theoretical support, we do not need to care how the noise-risk vector is calculated. This is because the regret is defined as a comparative difference between the total risk of actual selections and the total risk of the best selections (see Eq. (2)). The practical selection error (i.e., how much incorrectly labeled data we select) only depends on the absolute selection risk of the best k -set selection, which is decreased when we use some good noise-risk calculation (see Sec. 5.1).

4.1. Regret bound of TAKS

The regret bound of TAKS is directly derived from the following general theorem [4]:

Theorem 1 ([4]). *Let $k \in \{1, \dots, n-1\}$. By setting $\eta = \sqrt{kT}$ ¹, the regret of the adaptive k -set selection algorithm with FPL is upper bounded as follows:*

$$\mathbb{E}[R_T] \leq 2\sqrt{2kT \ln \binom{n}{k}}, \quad (3)$$

where the expectation comes from the randomness of FPL.

This theorem says that the regret, which is the performance difference between the selected k -sets and the best k -set, is bounded by a constant value given by T , n , and k , and the bound is not exploded with the huge $\binom{n}{k}$ choices of k -sets but just relative to $\sqrt{\ln \binom{n}{k}}$.

4.2. Selection risk bound of TAKS

Based on Theorem 1, which is a result for the general k -set selection problem, we now derive a new theoretical result specific to TAKS. Specifically, this theoretical result proves that TAKS select samples with a smaller noise-risk on average over $t = 1$ to T and therefore will give a more direct interpretation of how theoretical support of TAKS is beneficial for the sample selection. We define the average selection risk as $\text{ASR}_{(\mathbf{d}_1, \dots, \mathbf{d}_T)} = (1/T) \sum_{t=1}^T \mathbf{d}_t \cdot \boldsymbol{\theta}_t$ for the length T of sequences of selected samples $\mathbf{d}_1, \dots, \mathbf{d}_T$ and noise-level vectors $\boldsymbol{\theta}_1, \dots, \boldsymbol{\theta}_T$.

¹The parameter η is theoretically set as \sqrt{kT} , for guaranteeing the worst-case performance by using kT , i.e., the worst total selection risk. In practice, we can achieve much smaller regret by setting a smaller η . In our experiment, we set η like $\eta = 10^{-3}\sqrt{kT}$.

Corollary 2. *For a sequence of noise-risk vectors $\boldsymbol{\theta}_1, \dots, \boldsymbol{\theta}_T$, we assume that TAKS selects $\mathbf{d}_1, \dots, \mathbf{d}_T$ samples and the best k -set sample selection $\mathbf{d}^* = \arg \min_{\mathbf{d} \in \mathcal{D}} \sum_{t=1}^T \mathbf{d} \cdot \boldsymbol{\theta}_t$ achieves αk average selection risk (i.e., $\text{ASR}_{(\mathbf{d}^*, \dots, \mathbf{d}^*)} = \alpha k$), where $0 \leq \alpha \leq 1$. Then, $\text{ASR}_{(\mathbf{d}_1, \dots, \mathbf{d}_T)}$ is upper bounded as follows:*

$$\mathbb{E}[\text{ASR}_{(\mathbf{d}_1, \dots, \mathbf{d}_T)}] \leq \alpha k \left(\frac{2\sqrt{2 \ln n}}{\sqrt{T\alpha}} + 1 \right)$$

The proof is shown in supplementary materials.

The parenthesized term is more than 1 and it becomes closer to 1 when the fraction part is smaller. In other words, $\text{ASR}_{(\mathbf{d}_1, \dots, \mathbf{d}_T)}$ becomes αk when the fraction part is sufficiently small. The fraction part ($2\sqrt{2 \ln n}/\sqrt{T\alpha}$) is not so large when we use a large training sample set because the dependency on the sample size n is logarithmic, and thus that is a great advantage for the sample selection for DNN training which basically requires large training samples. Moreover, the fraction part becomes smaller with increasing T . Consequently, $\text{ASR}_{(\mathbf{d}_1, \dots, \mathbf{d}_T)}$ will get close to αk along with t . Since $\text{ASR}_{(\mathbf{d}_1, \dots, \mathbf{d}_T)}$ and αk are the average selection risks of TAKS and \mathbf{d}^* (i.e., the selection method that knows \mathbf{d}^* as an oracle), this conclusion proves that the DNN on TAKS can be trained with samples \mathbf{d}_t with as small noise-risk as \mathbf{d}^* .

5. Experimental Results

5.1. Noise-risk assessment

In this paper, we assess a noise-risk of x_i as follows:

$$\theta_{i,t} = \frac{1 - \text{is}(f_t(x_i) = y_i)p(f_t(x_i))}{2}, \quad (4)$$

where $f_t(x_i)$ is the predicted label of x_i . The function $\text{is}(\cdot)$ returns +1 if \cdot is true and returns -1 otherwise, and p denotes the probability (i.e., softmax output) for the predicted label $f_t(x_i)$. Eq. (4) is motivated on the following hypothesis: if the sample x_i is predicted as the class y_i with higher confidence, it should have a correct label, and if the sample is predicted as a class other than y_i with higher confidence, it should have an incorrect label.

The above noise-risk assessment is reasonable because of the following reasons. First, selecting samples based on the confidence has been commonly used in several existing sample selection methods (e.g., [7,34]). Second, it is known that DNN basically fits easy samples first [1], and that suggests that clean (and easy) samples have high confidence even in the earlier epochs. Finally, with Eq. (4) incorrectly labeled samples are basically difficult to learn, i.e., DNN is hard to increase the confidence of the incorrect class label. The preliminary experiment verifies the above, and thus the noise-risk assessment is reasonable, as shown in supplementary materials.

Table 1: Average test accuracy (%) over the last 10 epochs and training time .

(Dataset) Noise	Standard	F-correction	Decouple		Co-teaching		Co-teaching+		JoCoR		TAKS (Ours)	
	Acc	Acc	Acc	×T	Acc	×T	Acc	×T	Acc	×T	Acc	×T
(MNIST) Symmetric-20%	78.67	90.71	94.74	1.10	94.52	1.60	97.77	1.61	<i>97.88</i>	1.47	97.94	1.19
(MNIST) Symmetric-50%	51.22	77.36	66.77	1.46	89.50	1.59	95.67	1.67	<i>95.90</i>	1.49	97.17	0.97
(MNIST) Symmetric-80%	22.43	51.16	27.42	1.50	78.52	1.59	66.13	1.73	<i>88.53</i>	1.49	92.32	0.81
(MNIST) Asymmetric-40%	78.97	88.99	82.04	1.35	90.21	1.59	92.48	1.65	<i>93.91</i>	1.50	95.77	1.22
(CIFAR-10) Symmetric-20%	68.92	74.21	69.95	1.61	78.16	1.98	78.68	2.00	85.75	1.73	<i>83.90</i>	0.99
(CIFAR-10) Symmetric-50%	41.93	52.68	40.91	1.71	70.79	1.97	56.90	1.99	78.92	1.73	<i>76.83</i>	0.74
(CIFAR-10) Symmetric-80%	15.85	18.99	15.29	1.82	<i>26.54</i>	1.98	23.50	2.00	25.51	1.73	40.24	0.53
(CIFAR-10) Asymmetric-40%	69.23	69.64	69.10	1.51	<i>73.59</i>	1.99	68.45	2.00	76.13	1.74	73.43	1.04
(CIFAR-100) Symmetric-20%	35.51	36.04	33.82	1.75	44.03	1.97	49.24	1.99	53.10	1.73	<i>50.74</i>	0.93
(CIFAR-100) Symmetric-50%	17.31	21.14	15.81	1.82	34.96	1.97	40.26	2.00	43.28	1.73	<i>40.98</i>	0.68
(CIFAR-100) Symmetric-80%	4.25	7.48	4.03	1.90	<i>14.81</i>	1.97	13.99	2.00	12.90	1.72	16.03	0.52
(CIFAR-100) Asymmetric-40%	27.91	27.11	26.95	1.75	28.69	1.98	<i>34.30</i>	2.01	32.39	1.74	35.23	0.98
(Clothing1M) Best	67.62	67.34	68.32	1.97	68.37	1.99	68.51	1.99	70.30*	2.00	<i>70.28</i>	0.41
(Clothing1M) Last	66.05	66.73	67.69		68.12		68.51		<i>69.79*</i>		70.28	

· Acc: Test accuracy (%) averaged over five trials. The best test accuracy is indicated with **red bold** and the second is indicated with *blue italic*.

· ×T: Computation time increase from Standard. Computation time of F-correction is the same as Standard (i.e., ×T=1) and thus omitted.

· For Clothing1M, we showed the test accuracy in the epoch with the highest validation accuracy (Best) and in the last epoch (Last).

· (*) For JoCoR, we refer to the accuracy on Clothing1M in [34] because the hyperparameters were not suggested.

Table 2: Average label precision (%) (clean samples / selected samples) over the last 10 epochs.

Noise	Decouple			Co-teaching			Co-teaching+			JoCoR			TAKS (Ours)		
	M	C10	C100	M	C10	C100	M	C10	C100	M	C10	C100	M	C10	C100
S20	37.31	68.19	72.50	95.38	92.20	91.87	79.93	56.95	48.73	<i>98.14</i>	<i>96.83</i>	<i>95.91</i>	99.72	98.16	97.65
S50	31.83	40.44	43.37	89.78	82.65	80.11	49.32	5.64	25.34	<i>95.43</i>	<i>91.04</i>	<i>87.40</i>	99.66	93.16	91.24
S80	16.91	18.19	18.24	77.48	<i>36.41</i>	<i>48.71</i>	12.08	19.73	18.83	<i>88.19</i>	35.95	45.15	97.19	51.43	51.88
A40	52.65	68.57	56.91	93.52	86.79	62.15	79.97	79.58	36.87	<i>95.99</i>	87.94	<i>63.59</i>	99.11	<i>87.47</i>	68.41

· Clothing1M has no GT about noisy labels and thus it is impossible to show its label precision.

· M:MNIST, C10: CIFAR-10, C100: CIFAR-100. · S{20,50,80}: Symmetric-{20,50,80}%. A40: Asymmetric-40%.

5.2. Experimental setup

Datasets We follow the evaluation scenario of the state-of-the-art trials for noisy-labeled data. We, therefore, used four datasets, MNIST [15], CIFAR-10, CIFAR-100 [14], and Clothing1M [36] and applied symmetric noise [30] and asymmetric noise [24] to those datasets to the first three datasets, which have only clean labels. For symmetric noise, we randomly choose a certain percentage (20%, 50%, and 80%) of the training samples and replaced their original (i.e., clean) label with one of the other (i.e., incorrect) labels. For asymmetric noise, we replaced the original label with the label of a prespecified confusing class. Note that 40% of asymmetric noise actually means that 20% of the labels are flipped, because the noise is applied to only half of the classes in [34].

Clothing1M is a large dataset and widely used to evaluate the methods for learning with noisy labels [16, 34, 39]. It has no ground-truth about noisy labels, but its noise rate is estimated at about 40% [36, 39]. For preprocessing, we resized the image samples to 256×256 , cropped them at the center to size 224×224 , and normalized them.

Baselines Following [34], we compared TAKS with

five state-of-the-art sample selection methods: “F-correction” [24], “Decouple” [19], “Co-teaching” [7], “Co-teaching+” [40], and “JoCoR” [34]. We also compared TAKS with the standard training strategy (“Standard”) which uses the whole (noisy) training set.

Evaluation metrics We measured the following three metrics; test accuracy, label precision, and training time. Test accuracy represents the proportion of correctly classified samples among the test samples, by the trained DNN. Following [7, 34], we focused on average test accuracy over the last 10 epochs (of $T = 200$ epochs). Label precision shows the percentage of clean samples among the selected samples; higher label precision means more clean samples are used for training a DNN. Training time is the time taken to train a DNN. For F-correction, we exclude its (long) pre-processing time to estimate the label transition matrix for a fair comparison; consequently, its computation time becomes the same as Standard.

We repeated the experiments five times for all datasets except Clothing1M and calculated the average for each metric. For Clothing1M, we conducted an experiment once, and label precision is not given because it has no ground-

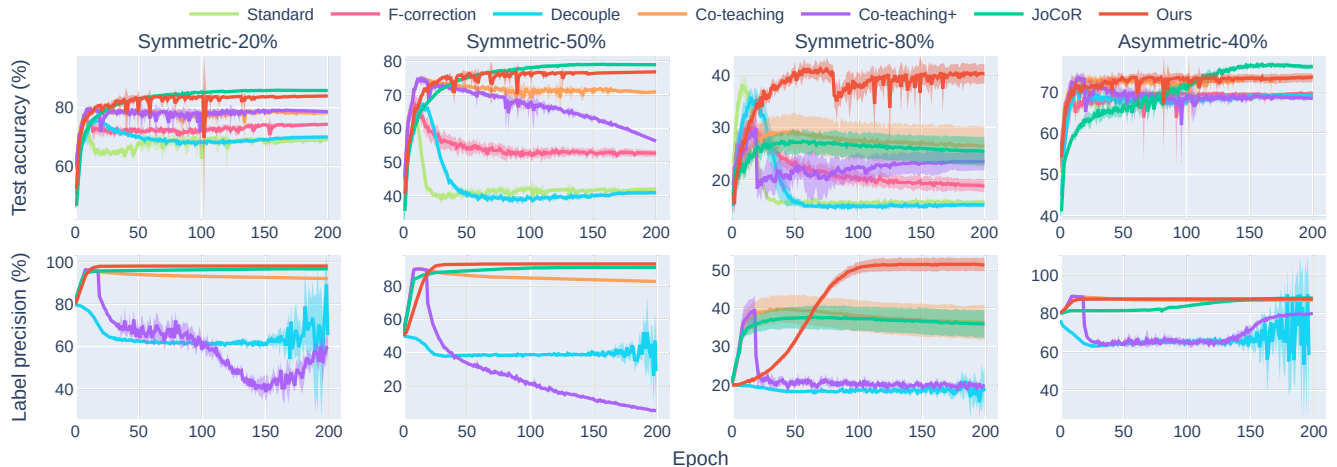


Figure 2: Test accuracy (Top) and label precision (Bottom) graphs with error band on CIFAR-10.

truth about noisy labels.

DNN structure and optimizer For a fair comparison, we follow the setup of JoCoR [34]. More details can be found in supplementary materials.

Hyperparameter search To fix the hyperparameters η and k , we split the noisy training samples into 80% noisy training samples and 20% *noisy validation samples*. With the validation samples, the best η was selected from its candidates $\eta \in \{10^{-4}, 5 \times 10^{-4}, 10^{-3}, 5 \times 10^{-3}\} \times \sqrt{kT}$.

The hyperparameter k should be fixed by using noise rate estimation. Although there are several techniques to estimate the noise rate [18, 41], it is still hard to estimate the true noise rate γ . Therefore, assuming that we could roughly estimate the noise rate as γ , we choose the best k from $\{1 - \gamma - 0.15, 1 - \gamma - 0.1, \dots, 1 - \gamma + 0.15\} \times n$ with the noisy validation samples.

Note that the above conditions are different from the state-of-the-art attempts and *disadvantageous* to TAKS. In fact, Co-teaching, Co-teaching+, and JoCoR use the true noise rate directly [7, 34, 40]. Furthermore, JoCoR searched for hyperparameters using *clean validation samples* [34]. We kept these conditions in our experiments. In contrast, hyperparameters of TAKS are searched by using the noisy validation samples and the rough estimation of γ . Although our hyperparameter search mimics a more practical scenario, it handicaps TAKS. The tuned hyperparameters are detailed in supplementary materials.

5.3. Experimental results

Classification performance Table 1 shows the average test accuracy over the last 10 epochs. For Clothing1M, it shows the test accuracy when the trained model achieved the best validation accuracy as “Best” and the test accuracy at the end of training as “Last” (by following [34]). TAKS achieved a noticeable performance improvement from Standard and, more importantly, outperformed all the other

baselines, achieving the best or second-best test accuracy in most cases. In particular, TAKS achieved significantly higher test accuracy than all other baselines when the training samples contained many incorrectly labeled samples, such as Symmetric-80%.

More precisely, TAKS achieved the highest test accuracy for all noise cases on MNIST. On CIFAR-10, TAKS and JoCoR performed better than the other baselines. However, in the Symmetric-80% case, the test accuracy of all baselines, including JoCoR, was significantly degraded from Symmetric-20% and 50%. On the other hand, TAKS still maintained higher test accuracy. Recall that its theoretical supports hold even in severely noisy cases, and TAKS can keep its reasonable performance if the sequence of the noise-risk vectors is given correctly. For Clothing1M, TAKS achieved the best accuracy in both the “Best” and “Last” scenarios. It is noteworthy again that our hyperparameters were determined in a more challenging scenario than the baselines, where the exact noise ratio and/or a clean validation set were used.

We also plotted the test accuracy curves on CIFAR-10 in Fig. 2 (Curves for other datasets can be found in the supplementary materials; most of the discussion below also applies to these datasets.). In most cases, the accuracy of Standard, F-correction, and Decouple increased and reached a high peak at the beginning when they learned general features. After that, they started overfitting the incorrectly labeled training samples, and the test accuracy dropped rapidly. In contrast, the other baselines and TAKS maintained high test accuracy. A closer observation reveals that the test accuracy of TAKS steadily increased while the test accuracy of the baselines gradually decreased for difficult cases, such as Symmetric-80%.

Label precision The robustness of TAKS can be explained with label precision. Table 2 shows the average label precision over the last 10 epochs. In all noise cases of all datasets

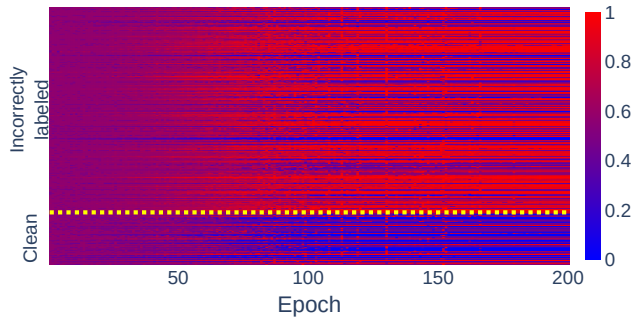


Figure 3: Change of noise-risk $\theta_{i,t}$ on CIFAR-10 in Symmetric-80%.

except for one, TAKS achieved the best label precision, and even in the one case, TAKS achieved the second-best. It means that TAKS avoided incorrectly labeled samples successfully and prevented the DNN from overfitting them.

Fig. 2 plots the label precision on CIFAR-10 at each epoch. In all cases, the label precision of TAKS did not decrease and rather kept increasing or saturating. Although high label precision does not directly guarantee high test accuracy, it surely confirms the high noise tolerance of TAKS. It was especially noticeable when there was much noise in the training sample, such as the Symmetric-80%. In the case, Fig. 2 shows that the test accuracy of the baselines, including Co-teaching and JoCoR, began to deteriorate as their label precision began to decrease. In contrast, the accuracy of TAKS has steadily increased, and even longer training is expected to lead to better performance.

Fig. 3 shows the change in the noise-risk $\theta_{i,t}$ of each training sample on CIFAR-10 with Symmetric-80% over the epochs. After the beginning epochs with almost uniform noise-risk values over all samples, most clean samples were properly distinguished by their small noise-risk values.

Fig. 4 shows the feature distributions in the Symmetric-80% case on CIFAR-10 by TAKS. UMAP [20] was used for two-dimensional visualization. Clean training samples of the same class form a cluster, whereas incorrectly labeled training samples tended to be scattered. This allowed TAKS to classify the clean test samples accurately. Fig. 4 also shows the feature distributions of the selected and the non-selected samples of TAKS. The samples belonging to the clusters for the clean samples were mainly selected, and most incorrectly-labeled samples outside of the clusters were not selected. This suggests that the noise-risk vectors worked successfully to exclude suspicious samples that were far from the cluster of clean samples.

Computation time It should be emphasized that TAKS is more efficient than the baselines. Table 1 shows the training time of each method and proves that TAKS was faster than the baselines in almost all cases. Moreover, TAKS was even faster than Standard in most cases, because TAKS uses only $k < n$ samples, whereas Standard uses all n samples. For

Table 3: Results of ablation study.

Noise	Greedy			Naive		
	M	C10	C100	M	C10	C100
S20	91.78	83.64	49.29	92.62	82.07	45.11
S50	88.22	76.96	38.08	89.28	66.65	21.85
S80	70.22	25.09	11.33	66.06	20.16	4.20
A40	92.24	71.65	33.26	89.84	69.12	33.10

- Gray cell indicates that it is less accurate than TAKS.
- See Table 2 for the notations, such as M and S20.

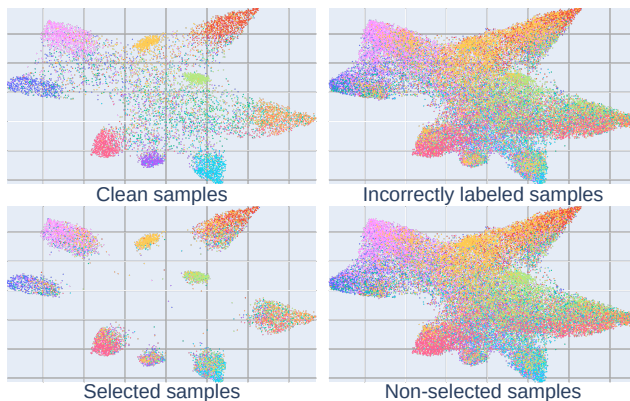


Figure 4: Visualization of the feature distribution of the noisy training samples, CIFAR-10 in Symmetric-80%, by TAKS. Colors represent classes. Incorrectly labeled samples are plotted with the color of their true class.

example, k became the smallest for Symmetric-80%, and thus, TAKS became twice and four times as fast as Standard and co-training methods, respectively.

5.4. Ablation study

To prove the effectiveness of FPL for a smaller total selection risk, we conduct an ablation study with the same settings as Sec. 5.2. More specifically, we compare FPL with the following two algorithms, “Greedy” and “Naive.” Greedy does not focus on *total* selection risk. Instead, it selects \mathbf{d}_t which minimizes $\mathbf{d}_t \cdot \boldsymbol{\theta}_{t-1}$ at every epoch t . This means Greedy trusts temporary noise-risk vector completely. Naive selects \mathbf{d}_t which minimizes $\sum_{\tau=1}^t \mathbf{d}_\tau \cdot \boldsymbol{\theta}_{\tau-1}$ at epoch t . That is, it selects the k -set that gives the current minimum total selection risk without the perturbation by r . Note that Naive corresponds to FTL [8]. Table 3 shows the average test accuracy of the above three methods over the last 10 epochs. By comparing between Tables 1 and 3, it is proved that TAKS outperforms the others. Especially, Greedy performed significantly worse than ours for high noise-rate data, because the noise-risk vector can be more unstable for noisier data. Naive fails in many cases because it has suffered from the unreliable noise-risk in early epochs. Ours can overcome these problems by the perturbation mechanism with the support of the lower regret bound.

6. Conclusion

We tackled the learning task from noisy-labeled data and proposed a novel DNN training method, TAKS, based on adaptive sample selection. The sample selection algorithm was inspired by an adaptive k -set selection, which allows TAKS to have strong theoretical support. In the experiments, we showed that the proposed method worked more efficiently and effectively than state-of-the-art methods. We observed the behaviors of the proposed method and confirmed that it could train DNNs while excluding the incorrectly-labeled samples appropriately.

References

- [1] Devansh Arpit, Stanislaw K Jastrzebski, Nicolas Ballas, David Krueger, Emmanuel Bengio, Maxinder S Kanwal, Tegan Maharaj, Asja Fischer, Aaron C Courville, Yoshua Bengio, et al. A closer look at memorization in deep networks. In *Proc. ICML*, 2017. 5
- [2] Lucas Beyer, Olivier J Hénaff, Alexander Kolesnikov, Xiao-hua Zhai, and Aäron van den Oord. Are we done with imagenet? *arXiv preprint arXiv:2006.07159*, 2020. 1
- [3] Markus M Breunig, Hans-Peter Kriegel, Raymond T Ng, and Jörg Sander. Lof: identifying density-based local outliers. In *Proc. SIGMOD*, 2000. 2
- [4] Alon Cohen and Tamir Hazan. Following the perturbed leader for online structured learning. In *Proc. ICML*, 2015. 3, 4, 5
- [5] Jia Deng, Wei Dong, Richard Socher, Li-Jia Li, Kai Li, and Li Fei-Fei. Imagenet: A large-scale hierarchical image database. In *Proc. CVPR*, 2009. 1
- [6] Benoît Fréney and Michel Verleysen. Classification in the presence of label noise: a survey. *TNNLS*, 25(5):845–869, 2013. 1
- [7] Bo Han, Quanming Yao, Xingrui Yu, Gang Niu, Miao Xu, Weihua Hu, Ivor Tsang, and Masashi Sugiyama. Co-teaching: Robust training of deep neural networks with extremely noisy labels. In *Proc. NeurIPS*, 2018. 2, 5, 6, 7
- [8] Elad Hazan. Introduction to online convex optimization. *Foundations and Trends in Optimization*, 2(3-4):157–325, 2016. 4, 8
- [9] Kaiming He, Xiangyu Zhang, Shaoqing Ren, and Jian Sun. Deep residual learning for image recognition. In *Proc. CVPR*, 2016. 11
- [10] Lu Jiang, Zhengyuan Zhou, Thomas Leung, Li-Jia Li, and Li Fei-Fei. Mentornet: Learning data-driven curriculum for very deep neural networks on corrupted labels. In *Proc. ICML*, 2018. 2
- [11] Adam Kalai and Santosh Vempala. Geometric algorithms for online optimization. *Journal of Computer and System Sciences*, 71(3):291–307, 2002. 4
- [12] Diederik P Kingma and Jimmy Ba. Adam: A method for stochastic optimization. In *Proc. ICLR*, 2015. 11
- [13] Wouter M Koolen, Manfred K Warmuth, and Jyrki Kivinen. Hedging structured concepts. In *Proc. COLT*, 2010. 3, 4
- [14] Alex Krizhevsky and Geoffrey Hinton. Learning multiple layers of features from tiny images. 2009. 2, 6
- [15] Yann LeCun, Corinna Cortes, and CJ Burges. Mnist handwritten digit database. 2010. 2, 6
- [16] Junnan Li, Yongkang Wong, Qi Zhao, and Mohan S Kankanhalli. Learning to learn from noisy labeled data. In *Proc. CVPR*, 2019. 6
- [17] Yuncheng Li, Jianchao Yang, Yale Song, Liangliang Cao, Jiebo Luo, and Li-Jia Li. Learning from noisy labels with distillation. In *Proc. CVPR*, 2017. 3
- [18] Tongliang Liu and Dacheng Tao. Classification with noisy labels by importance reweighting. *TPAMI*, 38(3):447–461, 2015. 7
- [19] Eran Malach and Shai Shalev-Shwartz. Decoupling “when to update” from “how to update”. In *Proc. NeurIPS*, 2017. 2, 6
- [20] Leland McInnes, John Healy, and James Melville. Umap: Uniform manifold approximation and projection for dimension reduction. *arXiv preprint arXiv:1802.03426*, 2018. 8
- [21] Aditya Menon, Brendan Van Rooyen, Cheng Soon Ong, and Bob Williamson. Learning from corrupted binary labels via class-probability estimation. In *Proc. ICML*, 2015. 3
- [22] David R Musser. Introspective sorting and selection algorithms. *Software: Practice and Experience*, 27(8):983–993, 1997. 4
- [23] Nagarajan Natarajan, Inderjit S Dhillon, Pradeep K Ravikumar, and Ambuj Tewari. Learning with noisy labels. In *Proc. NeurIPS*, 2013. 3
- [24] Giorgio Patrini, Alessandro Rozza, Aditya Krishna Menon, Richard Nock, and Lizhen Qu. Making deep neural networks robust to label noise: A loss correction approach. In *Proc. CVPR*, 2017. 3, 6
- [25] Mengye Ren, Wenyuan Zeng, Bin Yang, and Raquel Urtasun. Learning to reweight examples for robust deep learning. In *Proc. ICML*, 2018. 3
- [26] Filipe Rodrigues and Francisco Camara Pereira. Deep learning from crowds. In *Proc. AAAI*, 2018. 3
- [27] Yanyao Shen and Sujay Sanghavi. Learning with bad training data via iterative trimmed loss minimization. In *Proc. ICML*, 2019. 2
- [28] Daiki Suehiro, Kohei Hatano, Shuji Kijima, Eiji Takimoto, and Kiyohito Nagano. Online prediction under submodular constraints. In *Proc. ALT*, 2012. 3, 4
- [29] Sainbayar Sukhbaatar, Joan Bruna Estrach, Manohar Paluri, Lubomir Bourdev, and Robert Fergus. Training convolutional networks with noisy labels. In *Proc. ICLR*, 2015. 1
- [30] Brendan Van Rooyen, Aditya Menon, and Robert C Williamson. Learning with symmetric label noise: The importance of being unhinged. In *Proc. NeurIPS*, 2015. 6
- [31] Andreas Veit, Neil Alldrin, Gal Chechik, Ivan Krasin, Abhinav Gupta, and Serge Belongie. Learning from noisy large-scale datasets with minimal supervision. In *Proc. CVPR*, 2017. 3
- [32] Yisen Wang, Weiyang Liu, Xingjun Ma, James Bailey, Hongyuan Zha, Le Song, and Shu-Tao Xia. Iterative learning with open-set noisy labels. In *Proc. CVPR*, 2018. 2

- [33] Manfred K Warmuth and Dima Kuzmin. Randomized online PCA algorithms with regret bounds that are logarithmic in the dimension. *JMLR*, 9(Oct):2287–2320, 2008. [1](#), [3](#), [4](#)
- [34] Hongxin Wei, Lei Feng, Xiangyu Chen, and Bo An. Combating noisy labels by agreement: A joint training method with co-regularization. In *Proc. CVPR*, 2020. [2](#), [5](#), [6](#), [7](#)
- [35] Xiaobo Xia, Tongliang Liu, Nannan Wang, Bo Han, Chen Gong, Gang Niu, and Masashi Sugiyama. Are anchor points really indispensable in label-noise learning? In *Proc. NeurIPS*, 2019. [3](#)
- [36] Tong Xiao, Tian Xia, Yi Yang, Chang Huang, and Xiaogang Wang. Learning from massive noisy labeled data for image classification. In *Proc. CVPR*, 2015. [1](#), [2](#), [6](#)
- [37] Yan Yan, Rómer Rosales, Glenn Fung, Ramanathan Subramanian, and Jennifer Dy. Learning from multiple annotators with varying expertise. *Machine learning*, 95(3):291–327, 2014. [1](#)
- [38] Quanming Yao, Hansi Yang, Bo Han, Gang Niu, and James Tin-Yau Kwok. Searching to exploit memorization effect in learning with noisy labels. In *Proc. ICML*, 2020. [3](#)
- [39] Kun Yi and Jianxin Wu. Probabilistic end-to-end noise correction for learning with noisy labels. In *Proc. CVPR*, 2019. [6](#)
- [40] Xingrui Yu, Bo Han, Jiangchao Yao, Gang Niu, Ivor W Tsang, and Masashi Sugiyama. How does disagreement help generalization against label corruption? In *Proc. ICML*, 2019. [2](#), [6](#), [7](#)
- [41] Xiyu Yu, Tongliang Liu, Mingming Gong, Kayhan Batmanghelich, and Dacheng Tao. An efficient and provable approach for mixture proportion estimation using linear independence assumption. In *Proc. CVPR*, 2018. [7](#)
- [42] Xiyu Yu, Tongliang Liu, Mingming Gong, and Dacheng Tao. Learning with biased complementary labels. In *Proc. ECCV*, 2018. [1](#)
- [43] Chiyuan Zhang, Samy Bengio, Moritz Hardt, Benjamin Recht, and Oriol Vinyals. Understanding deep learning requires rethinking generalization. In *Proc. ICLR*, 2017. [1](#)

A. Proof of Corollary 2

Proof. For brevity, we simply use R_T as $\mathbb{E}[R_T]$. We first note that kT in Theorem 1 is used as a trivial upper bound of the total selection risk of the best k -set selection (i.e., $\sum_{t=1}^T \mathbf{d}^* \cdot \boldsymbol{\theta}_t \leq kT$ for any \mathbf{d}^* and $\boldsymbol{\theta}_1, \dots, \boldsymbol{\theta}_T$). By the assumption that the best k -set selection achieves αk selection risk, we replace kT with the actual total selection risk of the best selection αkT . Thus, the regret bound is rewritten as follows:

$$R_T \leq 2\sqrt{2\alpha kT \ln \binom{n}{k}}.$$

Applying $\binom{n}{k} \leq n^k$ for simplicity, we have the following:

$$R_T \leq 2\sqrt{2\alpha kT \ln n^k} = 2k\sqrt{2\alpha T \ln n}. \quad (5)$$

By the definition of regret, the average selection error in TAKS is written as follows:

$$\frac{1}{T} \sum_{t=1}^T \mathbf{d}_t \cdot \boldsymbol{\theta}_t = \frac{R_T}{T} + \frac{\sum_{t=1}^T \mathbf{d}^* \cdot \boldsymbol{\theta}_t}{T} = \frac{R_T}{T} + \alpha k$$

Applying the bound (5), we have the result:

$$\frac{1}{T} \sum_{t=1}^T \mathbf{d}_t \cdot \boldsymbol{\theta}_t \leq \frac{2k\sqrt{2\alpha T \ln n}}{T} + \alpha k = \alpha k \left(\frac{2\sqrt{2 \ln n}}{\sqrt{T\alpha}} + 1 \right).$$

Finally we take into account the randomness of FPL, we obtain the target bound. \square

B. Experimental details

B.1. Implementation

We implemented TAKS and baselines with PyTorch and the code of our implementation can be found from attachment. All experiments were conducted on NVIDIA 1080Ti.

B.2. Datasets

The detail of the datasets used in our experiments is shown in Table 4.

B.3. DNN structure and optimizer

The DNN architectures used on MNIST, CIFAR-10, and CIFAR-100 are shown in Table 5. We used a MLP with one hidden layer for MNIST, a CNN with six hidden layers for CIFAR-10 and CIFAR-100, and ResNet-18 [9] for Clothing1M. To optimize the DNN, we used Adam optimizer [12] ($\beta_1 = 0.9$ and $\beta_2 = 0.999$). For MNIST, CIFAR-10, and CIFAR-100, a learning rate was set to 10^{-3} up to 80 epochs and linearly decreased to $T = 200$ epochs to become 0 after that. For Clothing1M, the learning rate was set for each of five epochs as 8×10^{-4} , 5×10^{-4} , and 5×10^{-5} during 15 epochs. More details can be found in our code.

Table 4: The detail of datasets.

	#training	#test	#class
MNIST	60000	10000	10
CIFAR-10	50000	10000	10
CIFAR-100	50000	10000	100
Clothing1M	1000000	10526	14

Table 5: The detail of DNN architectures.

Target	MNIST	CIFAR-10 and CIFAR-100
Input	28×28	32×32
Hidden layer	fc, 256	3×3 conv, 64. BN 3×3 conv, 64. BN 2×2 max-pool
		3×3 conv, 128. BN 3×3 conv, 128. BN 2×2 max-pool
		3×3 conv, 196. BN 3×3 conv, 16. BN 2×2 max-pool
Output		fc, #class softmax

· ReLU was used as an activation function.

Table 6: Tuned η and k for each dataset.

	$\eta (\times \frac{\sqrt{kT}}{10000})$				$k (\times \frac{n}{100})$			
	M	C10	C100	CM	M	C10	C100	CM
S20	5	5	5		65	75	65	
S50	50	10	10		35	45	35	
S80	50	50	50	10	15	20	15	50
A40	10	5	5		70	80	70	

· See Table 6 for the notations, such as M and S20.

C. Noise-risk vector validation

The proposed noise-risk for x_i is

$$\theta_{i,t} = \frac{1 - \text{is}(f_t(x_i) = y_i)p(f_t(x_i))}{2},$$

where $f_t(x_i)$ is the predicted label of x_i . The function $\text{is}(\cdot)$ returns +1 if \cdot is true and returns -1 otherwise, and p denotes the probability (i.e., softmax output) for the predicted label $f_t(x_i)$. Since $(\text{is}(f_t(x_i) = y_i)p(f_t(x_i)))$ is in $[-1, 1]$, $\theta_{i,t}$ is in $[0, 1]$.

We experimentally verify that the total selection risk with $\boldsymbol{\theta}_1, \dots, \boldsymbol{\theta}_t$ given by the above is smaller when the selected samples are cleaner. In other words, we verify that if we achieve a small (total) selection risk, the selected samples should be (averagely) cleaner. We use MNIST training samples with 50% label-noise and consider 0.5n-set sample selection. In this experiment, we assume that we know which samples are incorrectly labeled. We consider five subsets of samples, each of which contains

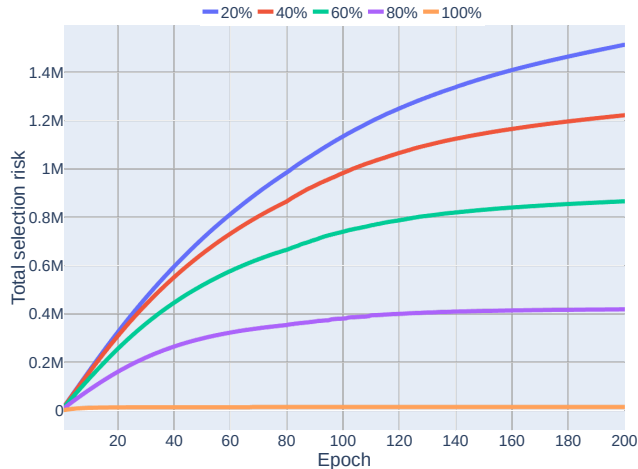


Figure 5: Total selection risk of sample selection for different clean sample ratios.

$\{20\%, 40\%, 60\%, 80\%, 100\%$ of clean samples. For simplicity, we fixed the IDs of selected samples and trained DNN with the samples on each rate (i.e., $\mathbf{d}_1, \dots, \mathbf{d}_T$ are the same at every epochs). Then, we compared the total risks corresponding to the subsets of samples. Fig. 5 shows the curves of the total selection risks along with the epochs, with $k = 0.5n$ on MNIST. We can see that the subsets of the selected samples containing smaller incorrectly labeled samples had smaller total selection risks. In particular, 100% clean subset of the samples achieved extremely low total selection risk compared to the others. Therefore, it is expected that we can train DNN with cleaner samples by aiming for smaller total selection risk.

D. Result details

D.1. Effect of η and k

Table 6 shows the tuned hyperparameters η and k . We can observe that the tuned η was never the smallest of the range for which we searched. It suggests that the perturbation \mathbf{r} plays an important role in finding cleaner samples. Moreover, it can be seen that the higher η was used for noisier cases of CIFAR-10 and CIFAR-100. It suggests that TAKS needs to have a larger perturbation to explore (minor) clean samples in cases with higher noise rates.

Table 6 also shows that the tuned k s were always less than or equal to the ideal k (that corresponds to the true noise rate) in all cases. This indicates that it is better to select a limited number of certainly clean samples while avoiding contamination by incorrectly labeled samples.

D.2. Test accuracy and label precision curves

Figs. 7, 8, and 9 show test accuracy and label precision curves on MNIST, CIFAR-10, and CIFAR-100, respec-

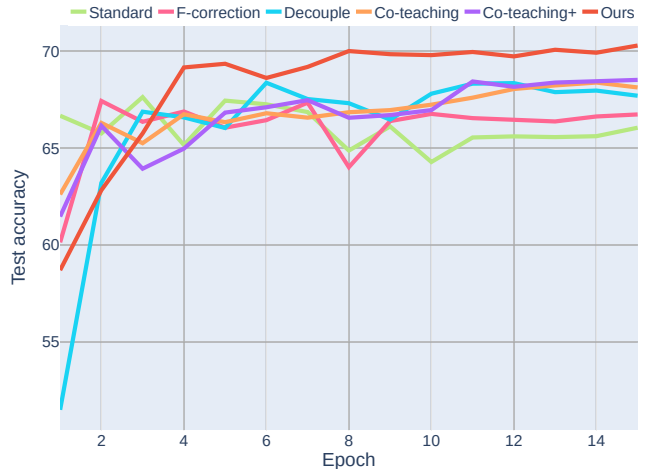


Figure 6: Test accuracy curves on Clothing1M.

tively. On most datasets, the test accuracy and label precision of TAKS kept increasing or saturating as the DNN was trained. On the other hand, in the Symmetric-80% case on MNIST and CIFAR-10, or in most cases on CIFAR-100, both test accuracy and label precision of baselines gradually decreased after they reached their peak.

Fig. 6 shows the test accuracy curves on Clothing1M. Note that, for Clothing1M, the results of JoCoR are not plotted because we could not reproduce the performance presented in their original paper due to the lack of hyperparameter value information, although we followed that JoCoR is trained for Clothing1M just by 15 epochs. Similar to other datasets, TAKS achieved the best test accuracy compared to the baselines. In addition, from getting the best performance at the end of the training, i.e., at the 15th epoch, we can expect to get better performance by training DNN with TAKS for a longer epoch.

D.3. Change of noise-risk

Figs. 10, 11, and 12 show the change of the noise-risk vector to each training sample along with epochs on MNIST, CIFAR-10, and CIFAR-100, respectively. On MNIST, the noise-risks of clean samples and incorrectly labeled samples were distinguished quickly. On CIFAR-10 and CIFAR-100, as the training sample contained more incorrectly-labeled samples, it became slower to distinguish between clean samples and incorrectly labeled samples, and relatively many samples are incorrectly distinguished. In particular, in the Symmetric-80% case on CIFAR-100, clean samples and incorrectly labeled samples were not well distinguished even up to 100 epochs. However, even in this case, the clean samples had smaller risk in the end, and TAKS could achieve higher precision than the baselines.

D.4. Feature distributions

Figs. 13, 14, and 15 visualize the feature distributions of TAKS on MNIST, CIFAR-10, and CIFAR-100, respectively, by UMAP. In the symmetric noise cases, incorrectly labeled samples tended to be scattered, and TAKS can ignore them successfully. In the asymmetric noise cases, TAKS selects most samples from the noiseless classes (e.g., “pink”, “violet-red”, “red”, “light-green”, and “dark blue” classes of CIFAR-10) and less samples from the noisy classes.

E. Future work

In future work, it would be interesting to design other effective noise-risk vector to estimate the noise-risk of samples more accurately. In addition, the idea of adaptive k -set selection could be applied to other learning tasks (e.g., ranking, regression, and detection) and datasets that contain noisy samples, such as samples from non-target classes and incomplete samples, rather than label noise.

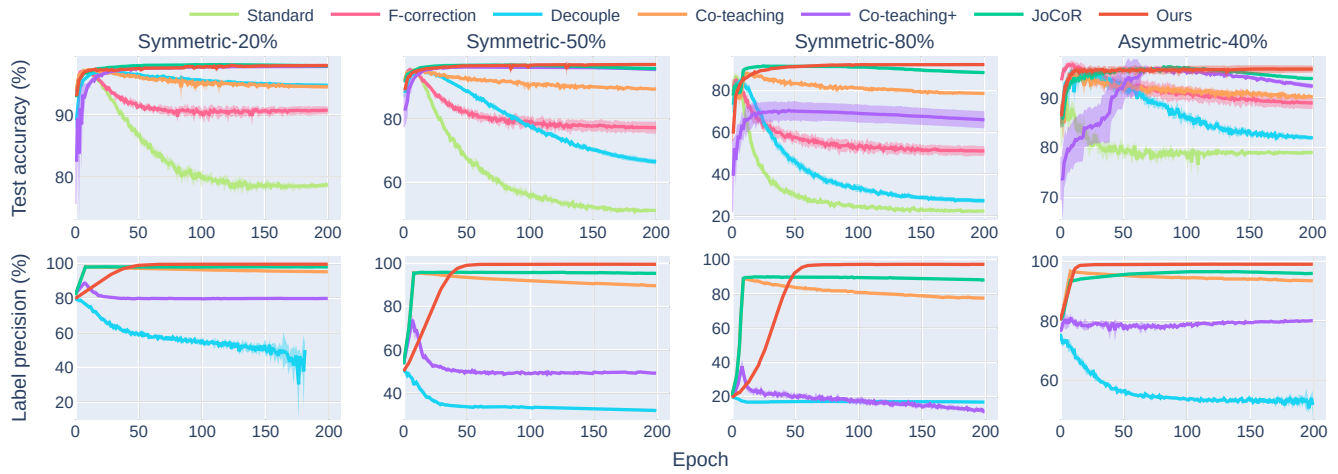


Figure 7: Test accuracy (Top) and label precision (Bottom) curves with error band on MNIST.

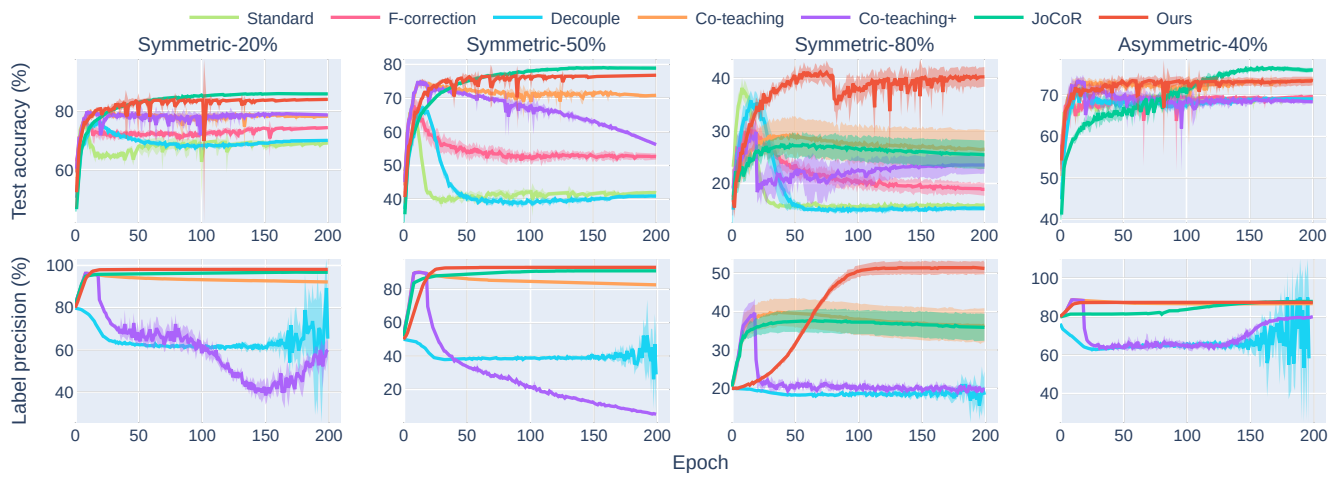


Figure 8: Test accuracy (Top) and label precision (Bottom) curves with error band on CIFAR-10.

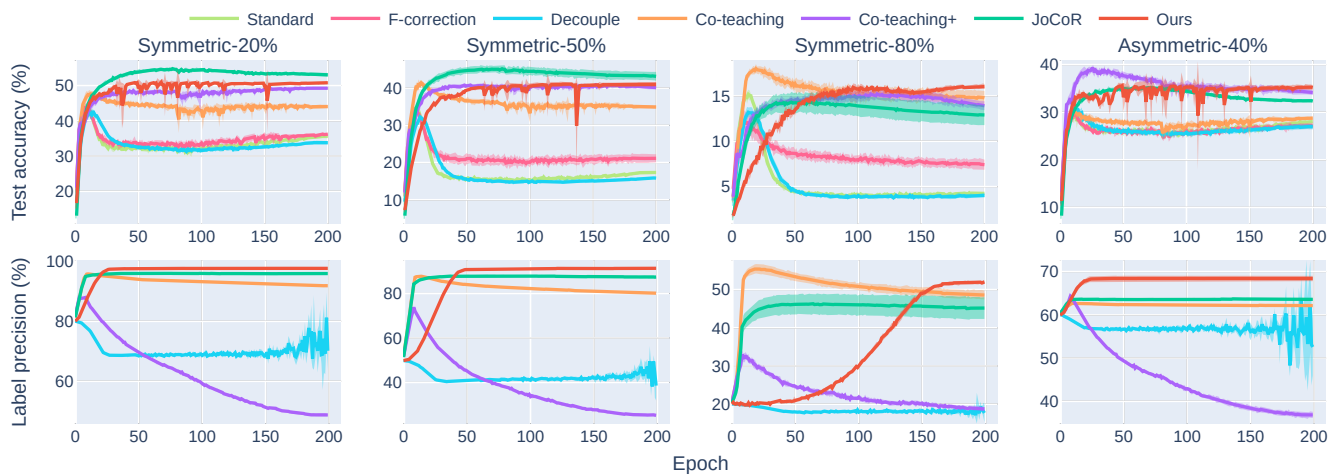


Figure 9: Test accuracy (Top) and label precision (Bottom) curves with error band on CIFAR-100.

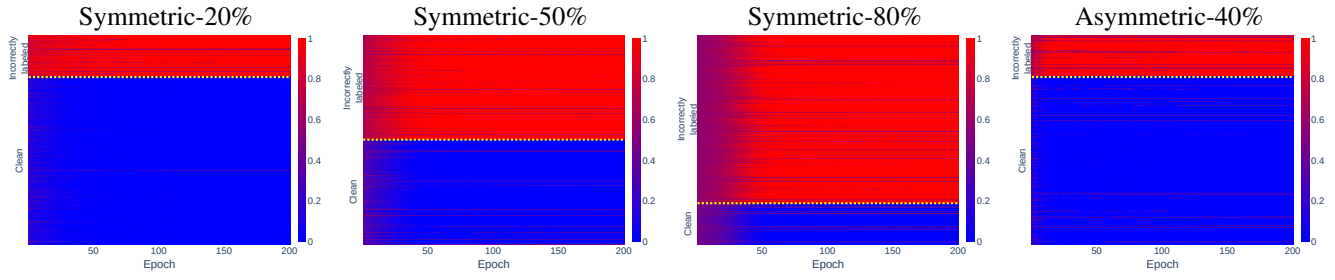


Figure 10: Estimated noise-risk on MNIST.

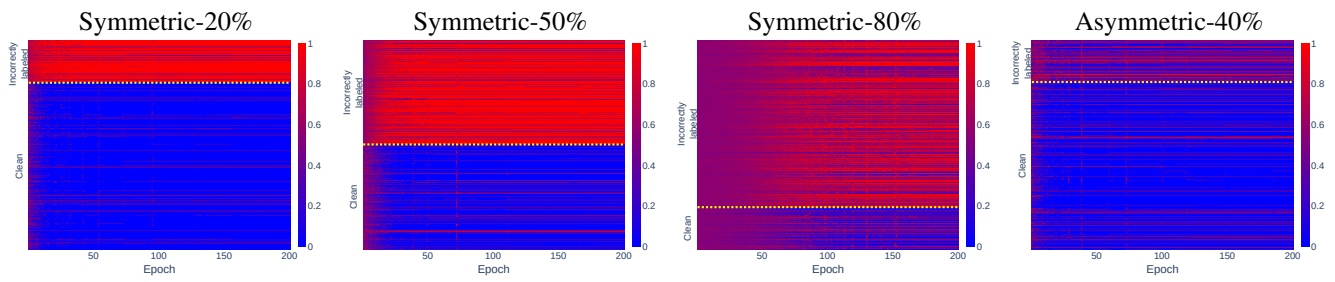


Figure 11: Estimated noise-risk on CIFAR-10.

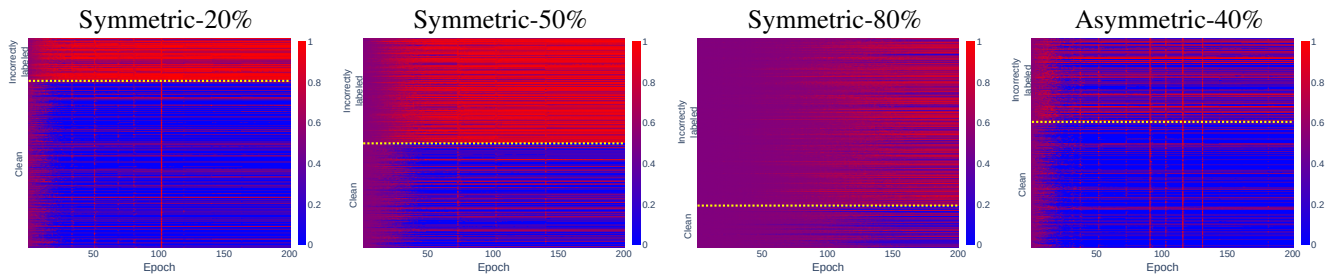


Figure 12: Estimated noise-risk on CIFAR-100.

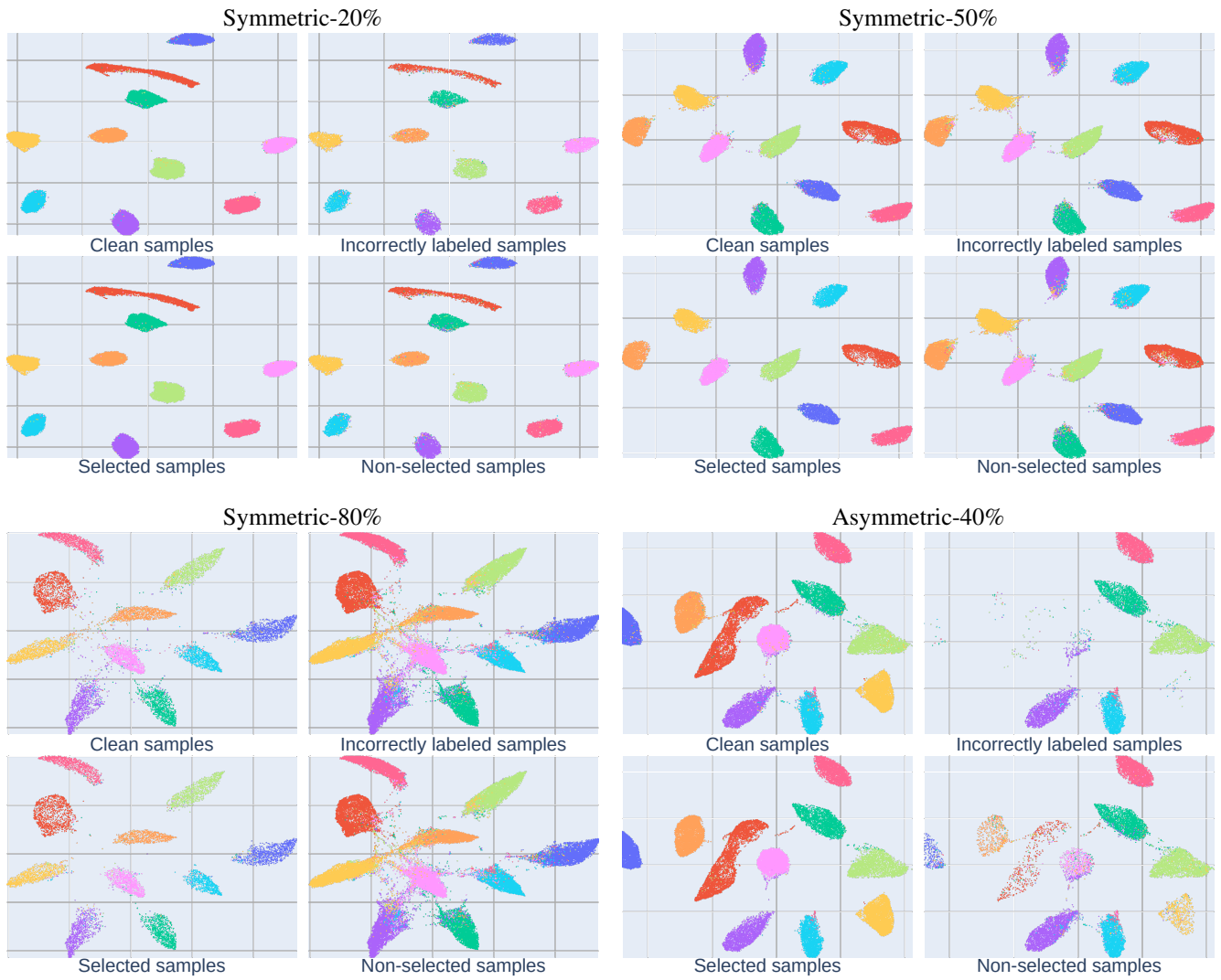


Figure 13: Visualization of the feature distribution of the noisy training samples on MNIST.

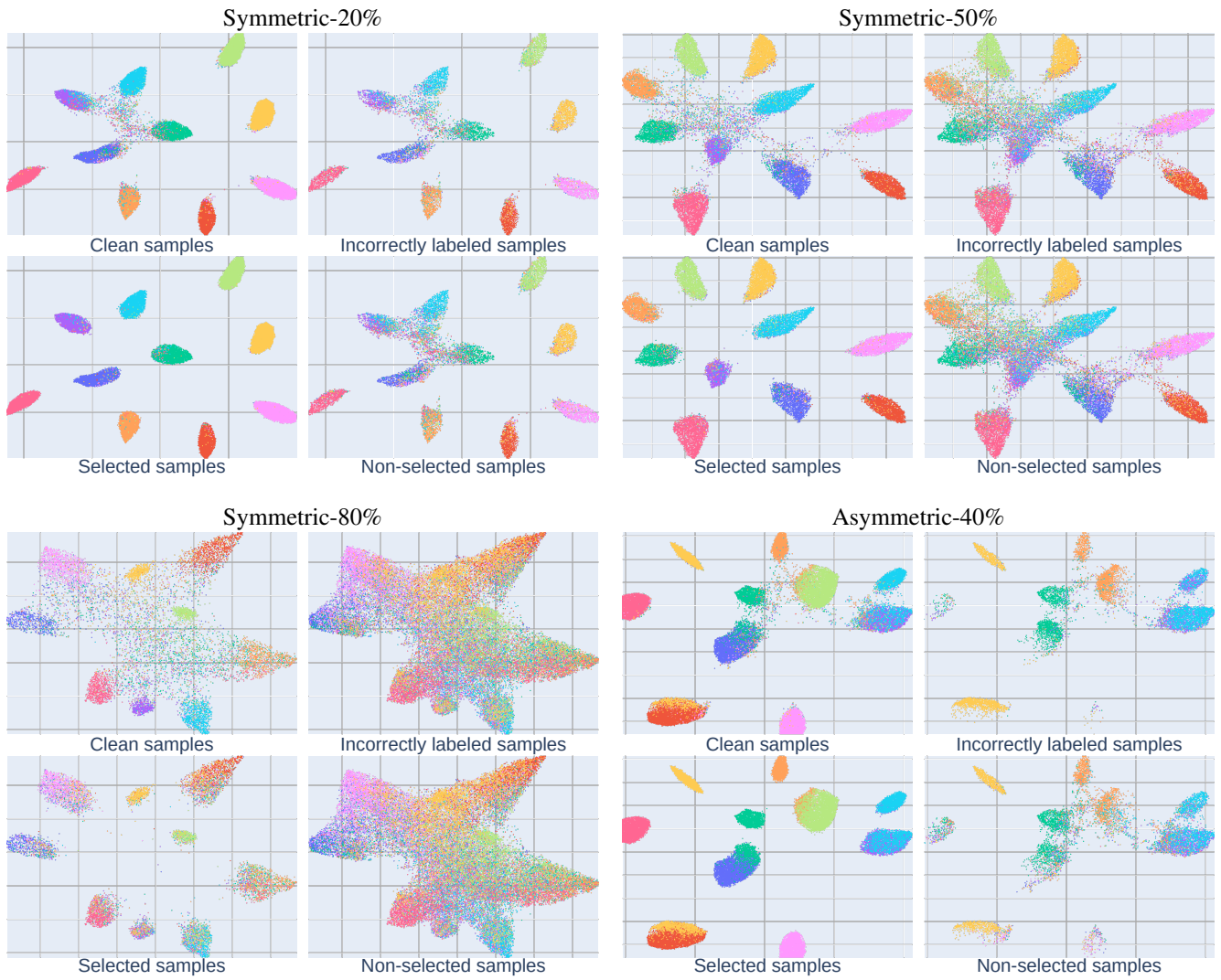


Figure 14: Visualization of the feature distribution of the noisy training samples on CIFAR-10.

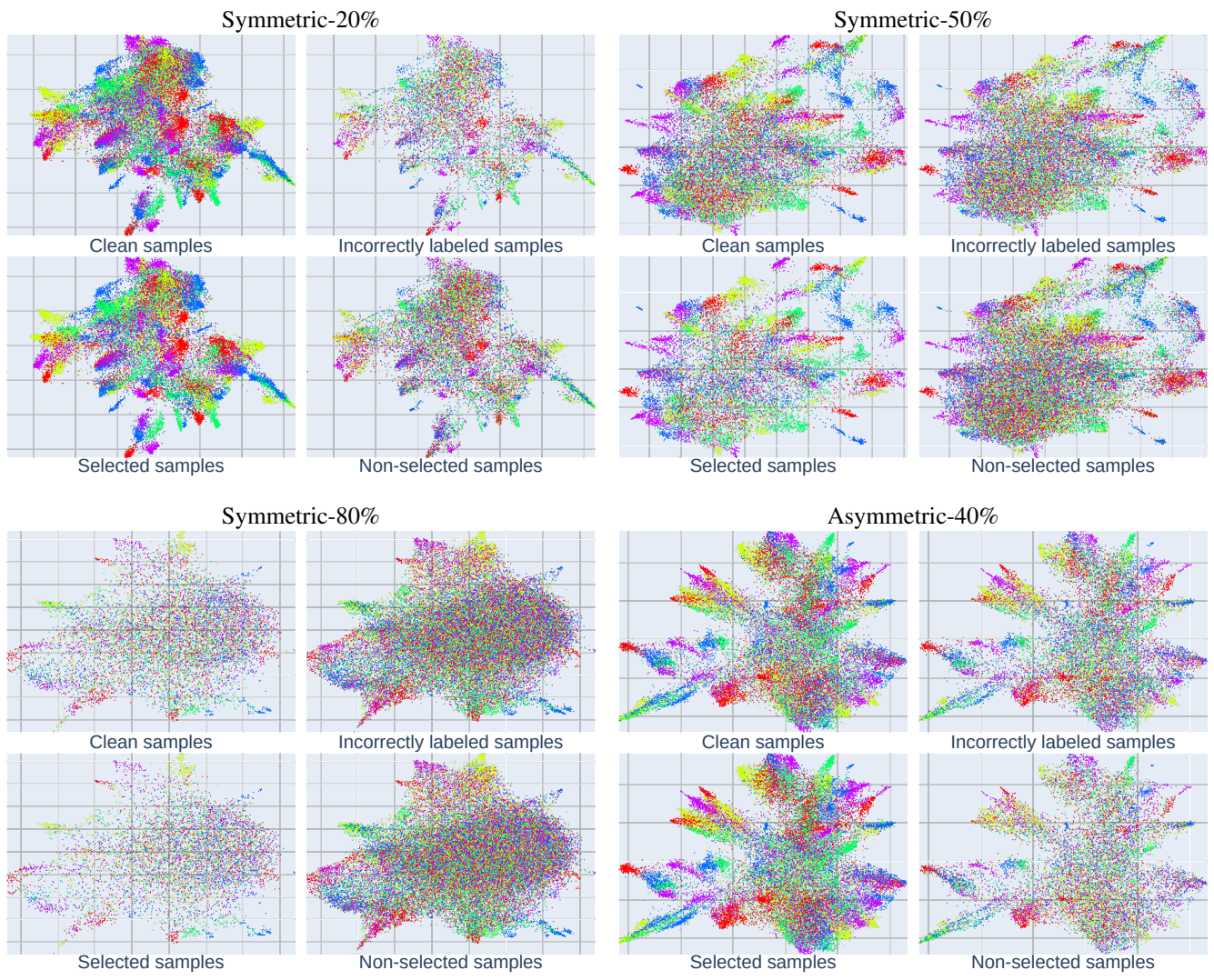


Figure 15: Visualization of the feature distribution of the noisy training samples on CIFAR-100.